Proceedings of the American Control Conference
Anchorage, AK May 8-10, 2002

Robust Nonlinear Control of the Electromagnetically Controlled Oscillator [1]

Harshad S. Sane
Corning-IntelliSense
36 Jonspin Rd., Wilmington, MA 01887
harshad@engin.umich.edu

Dennis S. Bernstein
Aerospace Engineering Department
Univ. of Michigan, Ann Arbor, MI 48109
dsbaero@umich.edu

Abstract

Most microelectromechanical systems are based on electromagnetic or electrostatic actuation forces. It is well known that linear controllers based on linearized models have a stable actuation range of one third of the nominal gap, while at larger displacements the electrostatic force dominates resulting in the electrodes pulling together. For Hammerstein systems with quadratic input nonlinearity we propose a nonlinear controller that guarantees stability and bounded disturbance rejection. For a single-sided electromagnetic oscillator we use this controller to achieve tracking. For a double-sided electromagnetic oscillator, we propose a control algorithm that achieves the desired performance while guaranteeing that the electromagnetic plates never pull together. These nonlinear controllers are robust since their stabilization and disturbance rejection properties do not require knowledge of the inertia, damping and stiffness of the plant.

1 Introduction

With breakthroughs in micro- and nano-engineering fabrication technologies, high performance microelectromechanical systems (MEMS) and nanoelectromechanical systems will be widely used in nano-computers, medicine, biotechnology, and other fields. Moreover, such systems are of great applicability in industrial applications such as optical networking devices [1, 12] using micro-opto-electromechanical systems (MOEMS), adaptive traction and slip control in automobiles using accelerometers and gyrosensors [2, 3, 10, 19, 20], micro-electromagnetic actuators, and hard-disk head precision control [4, 7, 8, 9].

Most electromechanical systems are based on electromagnetic or electrostatic actuation forces. Electromagnetic actuation is widely used in applications involving levitation, such as magnetically levitated vehicles and magnetic bearings [18]. Electrostatic actuation has also been studied for application to the control of large space antennas constructed of flexible membranes [11, 14].

It is well known [13, 17] that a voltage driven parallel plate has a stable actuation range of one third of the nominal gap, while at larger displacements the electrostatic force dominates the suspension restoring force and the electrodes pull together or 'snap'. Therefore, linear controllers based on linearized models are unstable at large deflection.

Here we consider the control of a spring-mass-damper system actuated by single- or double-sided electromagnetic or electrostatic forces. Double-sided actuation is commonly used in MEMS devices such as accelerometers, whereas single-sided actuation arises in the case of electrostatically controlled membranes, where double-sided control would block the transmission path. Single-sided actuation was considered in [6].

In Section 2 we present the dynamic model of a single-sided electromagnetically controlled oscillator (ECO) [5] and illustrate the problem of using linearized models to design linear controllers for stabilization at large deflections. In Section 3 we consider a Hammerstein plant with positive-real linear dynamics and quadratic input nonlinearity with an unknown constant disturbance. For this case, we construct a nonlinear controller that guarantees (Theorem 3.1) stability and asymptotic rejection of unknown disturbances. For the case of the single-sided ECO we employ these controllers to achieve asymptotic tracking or disturbance rejection.

In Section 4, we consider the case of double-sided actuation. Here we propose a control algorithm which achieves the desired performance guaranteeing that the electromagnetic plates never pull together or 'snap' at any time. We illustrate each controller using numerical examples. These nonlinear controllers are robust since their stabilization and disturbance rejection properties do not require knowledge of the inertia, damping and stiffness of the plant.

2 Single-Sided Electromagnetic Oscillator

Consider the single-sided electromagnetically controlled oscillator (ECO) shown in Figure 1. The dynamics of the oscillator (assumed to operate in the horizontal plane) [5] are given by

$$m\ddot{r} + c\dot{r} + kr = \frac{i^2}{(\bar{r} - r)^2}, \qquad (1)$$

[1] This research was supported in part by the Air Force Office of Scientific Research under grants F49620-98-1-0037 and F49620-01-1-0094.

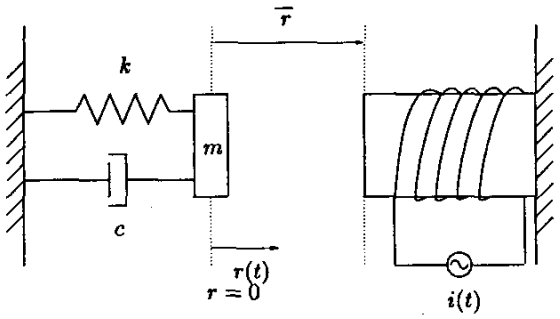

Figure 1: Schematic of the single-sided ECO.

where m is the mass, c is the damping constant, k is the spring constant, $i(t)$ is the commandable current supplied to the electromagnet, $r(t)$ is the position of the mass with the origin $r = 0$ chosen to coincide with the position of the mass when $i(t) = 0$ and the spring is relaxed, and the nominal gap $\bar{r}$ is the location of the electromagnet. Thus $r(t) = \bar{r}$ denotes contact between the mass and electromagnet.

Consider the problem of stabilizing the electromagnet at a non-zero equilibrium position $r = r_{eq}$, where $r_{eq} < \bar{r}$. The forced equilibrium position $r = r_{eq}$ of the equation of motion (1) satisfies

$$kr_{eq} = \frac{i_{eq}^2}{(\bar{r} - r_{eq})^2}, \tag{2}$$

where i_{eq} is the current needed to maintain the mass at the location $r = r_{eq}$. To translate the equilibrium point r_{eq} to the origin of a new coordinate system, let $\xi(t) \triangleq r(t) - r_{eq}$. Then the equation of motion (1) can be written in state space form as

$$\begin{bmatrix} \dot{\xi} \\ \ddot{\xi} \end{bmatrix} = \begin{bmatrix} 0 & 1 \\ -\frac{k}{m} & -\frac{c}{m} \end{bmatrix} \begin{bmatrix} \xi \\ \dot{\xi} \end{bmatrix} + \begin{bmatrix} 0 \\ \frac{1/m}{(\bar{r}-r_{eq}-\xi)^2} \end{bmatrix} \tilde{u} - \begin{bmatrix} 0 \\ \frac{kr_{eq}}{m} \end{bmatrix}, \tag{3}$$

where $\tilde{u}(t) = i^2(t)$. The linearization of (3) about the origin and $\tilde{u}(t) \equiv i_{eq}^2$ is given by

$$\dot{x}(t) = \begin{bmatrix} 0 & 1 \\ -\frac{k}{m}\frac{(\bar{r}-3r_{eq})}{(\bar{r}+a-r_{eq})} & -\frac{c}{m} \end{bmatrix} x(t) + \begin{bmatrix} 0 \\ \frac{1}{m(\bar{r}-r_{eq})^2} \end{bmatrix} \delta\tilde{u}(t), \tag{4}$$

where $x = [\delta\xi(t) \;\; \delta\dot{\xi}]^{\mathrm{T}}$ and $\delta\xi(t)$ and $\delta\tilde{u}(t)$ represent incremental variations in $\xi(t)$ and $\tilde{u}(t)$. From (4) it can be seen that the forced equilibrium position r_{eq} corresponding to i_{eq} is asymptotically stable if and only if $r_{eq} < \frac{1}{3}\bar{r}$.

The transition of the system from stability to instability can also be understood by examining potential functions. The total potential function V_{PE} can be written in non-dimensional form as

$$V_{PE} = \frac{1}{2}\left(\frac{r}{\bar{r}}\right)^2 - \left(\frac{r_{eq}}{\bar{r}}\right)\frac{(1-\frac{r_{eq}}{\bar{r}})^2}{1-\frac{r}{\bar{r}}}. \tag{5}$$

Note that $\frac{dV_{PE}}{dr}|_{r=r_{eq}} = 0$ and $\bar{r}^2(1-\frac{r_{eq}}{\bar{r}})\frac{d^2V_{PE}}{dr^2}|_{r=r_{eq}} = 1 - 3\frac{r_{eq}}{\bar{r}}$. When $r_{eq} < \frac{1}{3}\bar{r}$ the potential function has a local minimum at r_{eq} in a basin of stability. As r_{eq} becomes larger, the basin becomes smaller and eventually disappears, rendering the system unstable.

3 Nonlinear Control with Single-Sided Electromagnetic Actuation

In order to develop controllers for the single-sided ECO presented in Section 2, we consider the case of a Hammerstein system with quadratic input nonlinearity. Consider the SISO plant

$$\dot{x} = Ax + B(u^2 + d), \tag{6}$$
$$y = Cx, \tag{7}$$

with scalar control input $u \in \mathbf{R}$, scalar measurement $y \in \mathbf{R}$, and bounded disturbance $d \in \mathbf{R}$ satisfying $d(t) \leq 0$ for $t \geq 0$. Assume that (A, B, C) is minimal and positive real. Next, consider the controller

$$\dot{x_c} = A_c x_c + B_c(-C_c x_c)y, \tag{8}$$
$$\dot{\hat{a}} = \begin{cases} -Ky\hat{a}^{3/2} & \text{if } y \leq 0 \\ 0 & \text{if } y \geq 0 \end{cases}, \quad \hat{a}(0) > 0, \tag{9}$$
$$u = \sqrt{\hat{a}(1 - \mathrm{sign}(y))/2 + (C_c x_c)^2}, \tag{10}$$

where $\hat{a} \in \mathbf{R}$ and $K > 0$. Assume that (A_c, B_c, C_c) is minimal and strictly positive real.

Theorem 3.1 Consider the closed-loop system (6)-(10). Then $x(t), x_c(t) \to 0$ as $t \to \infty$. Furthermore, $\hat{a}(t)$ is bounded for all $t \geq 0$ and $\inf_{t\geq 0} \hat{a}(t) > 0$.

Proof: Let $a > 0$ satisfy $|d(t)| < a$ for all $t \geq 0$, and consider the Lyapunov candidate

$$V(x, x_c, \hat{a}) = x^{\mathrm{T}}Px + x_c^{\mathrm{T}}P_c x_c + \frac{1}{K}\left(\sqrt{\hat{a}} + \frac{a}{\sqrt{\hat{a}}}\right).$$

It can be shown that $\dot{V} \leq 0$ for all $t \geq 0$. The result follows using the invariant set theorem. For details see [15, 16]. ■

The controller (8)-(10) does not require any knowledge of the plant parameters. It is, however, required that (A, B, C) be positive real. In order to apply Theorem 3.1 to the single-sided ECO shown in Figure 1, we assume that the state $x = [\xi \;\; \dot{\xi}]^{\mathrm{T}}$ is available for feedback and let $y = Cx$ with $C = [1 \;\; 1]$. This renders the system $\left(\begin{bmatrix} 0 & 1 \\ -k & -c \end{bmatrix}, \begin{bmatrix} 0 \\ 1 \end{bmatrix}, C\right)$ strictly positive real. Next, with $i = u(\bar{r} - r_{eq} - \xi)$, (3) has the same form as (6) with $d = -kr_{eq}$.

For simulation purposes we consider $m = 1$, $k = 16.0$, $c = 4.0$, and $\bar{r} = 2.0$. For controller (8)-(10) we choose

$K = 10$ and

$$A_c = \begin{bmatrix} -12.5 & -40.5 & -36 \\ 1 & 0 & 0 \\ 0 & 1 & 0 \end{bmatrix}, \quad B_c = \begin{bmatrix} 1 \\ 0 \\ 0 \end{bmatrix},$$
$$C_c = [1 \quad 6.5 \quad 9]. \tag{11}$$

For a constant command input $r_{eq} = 1.0$, it can be seen in Figure 3 that the controller stabilizes the plant and follows the command input. Furthermore, $\hat{a}$ converges (not shown) as $t \to \infty$. Next, we consider a square wave command with a period of 12.5 seconds. Figures 3 and 3 show that the controller is able to drive the tracking error ξ to zero. Note that both values of the command input are beyond $r = \bar{r}/3$ and hence the forced equilibria of the system at these points are unstable as shown in Section 2.

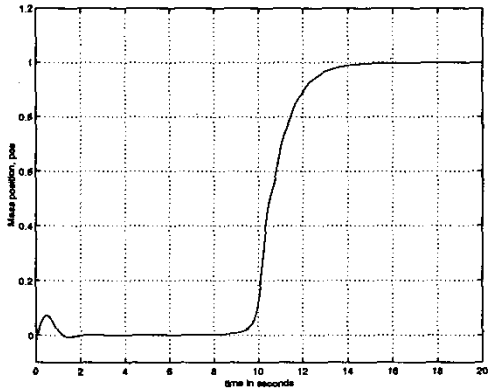

Figure 2: Mass position of the single-sided ECO with a constant position command $r_{eq} = 1.0$.

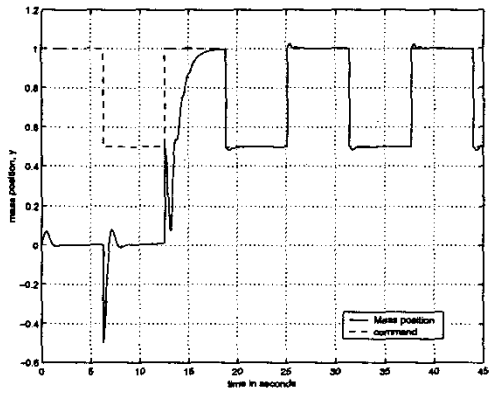

Figure 3: Mass position of the single-sided ECO with a time-varying position command. The position command in this case (dashed line) is a square wave of amplitude 0.75 and period 12.5 seconds. Note that both values of the square input correspond to unstable forced equilibria.

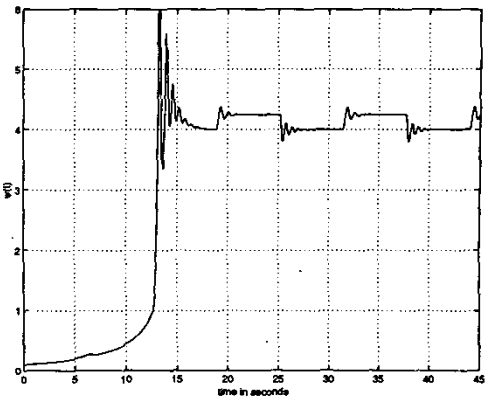

Figure 4: Time history control input u corresponding to the closed-loop response shown in Figure 3.

4 Double-Sided Electromagnetic Oscillator

In this section we consider the double-sided electromagnetically controlled oscillator (ECO) shown in Figure 5. The equation governing the motion for such a system is of the form

$$m\ddot{r} + c\dot{r} + kr = -f_d + \frac{i_1^2}{\gamma_1(\bar{r} - r)^2} - \frac{i_2^2}{\gamma_2(\bar{r} + r)^2} \tag{12}$$

where m is the mass of the oscillator, c is the damping constant, k is the spring constant, i_1 and i_2 are the currents in the electromagnets and γ_1, γ_2 are constants corresponding to each electromagnet. Let $\alpha_1 \triangleq \gamma_1 m$, $\alpha_2 \triangleq \gamma_2 m$. Here $f_d(t)$ is a bounded external force disturbance such that there exists $\alpha_3 > 0$ satisfying $|f_d(t)| < \alpha_3$ for all $t \geq 0$. When (12) models a MEMS accelerometer, the force f_d is due to the inertial acceleration sensed by the accelerometer.

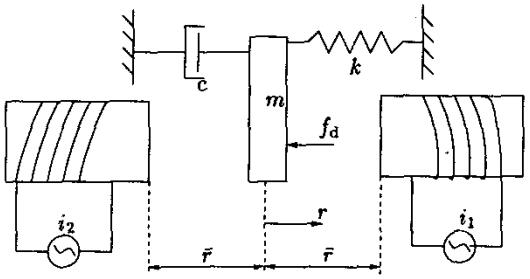

Figure 5: Schematic of the double-sided ECO.

In the following analysis we assume that m, c, k, γ_1, γ_2, and α_3 are unknown. However, we assume that $\alpha_1 = \gamma_1 m$ and $\alpha_2 = \gamma_2 m$ are positive and the nominal gap $\bar{r}$ is known. We further assume that both r and $\dot{r}$ are available for measurement. For the following theorem, let $a_1 \in \mathbf{R}$

and $a_2 \in \mathbf{R}$ be positive and define the Hurwitz matrix $A \triangleq \left[\begin{smallmatrix} 0 & 1 \\ -a_2 & -a_1 \end{smallmatrix}\right]$. Let $R \in \mathbf{R}^{2\times 2}$ be a positive definite matrix and let $P \triangleq \left[\begin{smallmatrix} P_1 & P_{12} \\ P_{12} & P_2 \end{smallmatrix}\right]$ be the solution of the Lyapunov equation $A^{\mathrm{T}}P + PA = -R$. Let $a > 0$ and let $\hat{c}$, $\hat{k}$, $\hat{\alpha}_1$, $\hat{\alpha}_2$, and $\hat{\alpha}_3$ be the estimates of the c/m, k/m, α_1, α_2 and α_3, respectively.

Theorem 4.1 Consider the dynamical system (12), assume $r(0) \in (-\bar{r}, \bar{r})$ and let $a > 0$. Next, consider the parameter update laws

$$\dot{\hat{c}} = -(P_{12}r + P_2\dot{r})\dot{r}, \tag{13}$$

$$\dot{\hat{k}} = -(P_{12}r + P_2\dot{r})r, \tag{14}$$

$$\dot{\hat{\alpha}}_1 = -k_1|v|(P_{12}r + P_2\dot{r})\hat{\alpha}_1^{3/2}, \tag{15}$$

$$\dot{\hat{\alpha}}_2 = k_2|v|(P_{12}r + P_2\dot{r})\hat{\alpha}_2^{3/2}, \tag{16}$$

$$\dot{\hat{\alpha}}_3 = |P_{12}r + P_2\dot{r}|\hat{\alpha}_3^{3/2}, \tag{17}$$

and let control inputs i_1 and i_2 given by

$$i_1 = (\bar{r} - r)\sqrt{k_1\hat{\alpha}_1|v|}, \tag{18}$$

$$i_2 = (\bar{r} + r)\sqrt{k_2\hat{\alpha}_1|v|}, \tag{19}$$

where

$$v \triangleq (\hat{c}-a_1)\dot{r}+(\hat{k}-a_2)r-\hat{\alpha}_3\,\mathrm{sign}(P_{12}r+P_2\dot{r})-\frac{P_{12}r+P_2\dot{r}}{(\bar{r}-r)(\bar{r}+r)^{3/2}}, \tag{20}$$

and

$$\begin{aligned} k_1 = a, k_2 = a+1 \quad \text{if} \quad v < 0, \\ k_1 = a+1, k_2 = a \quad \text{if} \quad v \geq 0. \end{aligned} \tag{21}$$

Then $r(t), \dot{r}(t) \to 0$ as $t \to \infty$. Furthermore, $r(t) \in (-\bar{r}, \bar{r})$ for $t \geq 0$ and $\dot{r}(t)$, $\hat{c}$, $\hat{k}$, $\hat{\alpha}_1$, $\hat{\alpha}_2$, and $\hat{\alpha}_3$ are bounded for all $t \geq 0$. Furthermore $\inf_{t\geq 0}\hat{\alpha}_1 > 0$, $\inf_{t\geq 0}\hat{\alpha}_2 > 0$ and $\inf_{t\geq 0}\hat{\alpha}_3 > 0$.

Proof: Using (18)-(21), (12) becomes

$$\begin{aligned} \ddot{r} = {} & -a_1\dot{r} - a_2 r + \hat{\alpha}_3\,\mathrm{sign}(P_{12}r + P_2\dot{r}) - f_{\mathrm{d}} \\ & + (\hat{c} - c/m)\dot{r} + \left(\hat{k} - k/m\right)r + k_1\frac{\hat{\alpha}_1 - \alpha_1}{\alpha_1}|v| \\ & - k_2\frac{\hat{\alpha}_2 - \alpha_2}{\alpha_2}|v| - \frac{P_{12}r + P_2\dot{r}}{(\bar{r} - r)(\bar{r} + r)^{3/2}}. \end{aligned} \tag{22}$$

Let $\tilde{x} \triangleq [r, \dot{r}, \hat{c}, \hat{k}, \hat{\alpha}_1, \hat{\alpha}_2, \hat{\alpha}_3]^{\mathrm{T}}$ and consider the Lyapunov candidate function $V : (-\bar{r}, \bar{r}) \times \mathbf{R}^3 \times [0,\infty)^3 \to [0, \infty)$

$$\begin{aligned} V(\tilde{x}) = {} & x^{\mathrm{T}}Px + (\hat{c} - \frac{c}{m})^2 + (\hat{k} - \frac{k}{m})^2 + \sum_{i=1,3}\frac{4}{\alpha_i}\left(\sqrt{\hat{\alpha}_i} + \right. \\ & \left. \frac{\alpha_i}{\sqrt{\hat{\alpha}_i}}\right) + 4P_{12}P_2(V_0(r) - V_0(0)), \end{aligned} \tag{23}$$

where $x = [r\ \dot{r}]^{\mathrm{T}}$ and $V_0(r)$ is defined by

$$V_0(r) \triangleq \frac{1}{\sqrt{2\bar{r}}}\left[\bar{r}\tanh^{-1}\left(\sqrt{\frac{r+\bar{r}}{2\bar{r}}}\right) + \bar{r}\sqrt{\frac{2\bar{r}}{r+\bar{r}}}\right]. \tag{24}$$

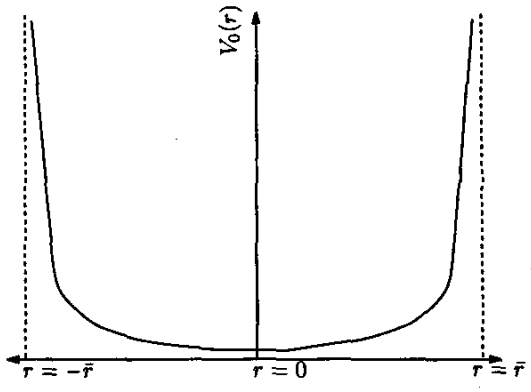

Figure 6: Lyapunov well $V_0(r)$ defined by (24).

Note that $V(\tilde{x})$ is unbounded as $r \to \pm\bar{r}$ and $\alpha_i \to 0$. Next, $\dot{V}_0(r)$ is given by

$$\dot{V}_0(r) = \frac{r\dot{r}}{(\bar{r}+r)^{3/2}(\bar{r}-r)}. \tag{25}$$

Using (13)-(17), (20), (24) and (25), the derivative of $V(\tilde{x})$ along the closed-loop trajectories is given by

$$\dot{V}(\tilde{x}) \leq -x^{\mathrm{T}}Rx - 2\frac{P_{12}^2r^2 + P_2^2\dot{r}^2}{(\bar{r}-r)(\bar{r}+r)^{3/2}}. \tag{26}$$

Using the invariant set theorem, it follows that $r, \dot{r} \to 0$ as $t \to \infty$. Furthermore, since $V(\tilde{x})$ is non-increasing along the closed-loop trajectories, it follows that all terms in (23) are bounded. Therefore, $\hat{c}$, $\hat{k}$, $\hat{\alpha}_1$, $\hat{\alpha}_2$, and $\hat{\alpha}_3$ are bounded for all $t \geq 0$. Since $V(\tilde{x})$ is unbounded as $r \to \pm\bar{r}$ and $\hat{\alpha}_i \to 0$, it follows that (refer to Remark 4.1 for brief explanation) $\inf_{t\geq 0}\hat{\alpha}_1 > 0$, $\inf_{t\geq 0}\hat{\alpha}_2 > 0$ and $\inf_{t\geq 0}\hat{\alpha}_3 > 0$. Furthermore, since $r(0) \in (-\bar{r}, \bar{r})$ it follows that $\inf_{t\geq 0} r > -\bar{r}$ and $\sup_{t\geq 0} r < \bar{r}$. ■

Remark 4.1 Consider a state $x \in \mathbf{R}$ of a dynamical system $\dot{\tilde{x}} = f(\tilde{x})$, which is known (or required to be) confined to an open interval $(a, b) \subset \mathbf{R}$ and has a nominal value of x_0. Let $V(\tilde{x})$ be a positive-definite LF satisfying $\dot{V}(\tilde{x}) \leq 0$ along the trajectories of the dynamical system. A *Lyapunov well* [15, 16] is a continuous function $V_{x_0} : (a, b) \to (0, \infty)$ which is unbounded at the boundaries of a confinement set (a, b). Now, suppose $V(\tilde{x}) = V_1(\tilde{x}) + V_{x_0}(x)$ where $V_1(\tilde{x}) > 0$. As $\dot{V}(\tilde{x}) \leq 0$, the invariance principle guarantees boundedness of state $\tilde{x}$. Since the Lyapunov well is positive definite, boundedness of $V(\tilde{x})$ ensures boundedness of $V_{x_0}(x)$. This implies that $x(t) \in (a, b)$ for all time. In (23), the terms corresponding to $\hat{\alpha}_1$, $\hat{\alpha}_2$, and $\hat{\alpha}_3$ are Lyapunov wells 'restricting' the corresponding variables to $[0, \infty)$. The term $V_0(r)$ serves as a Lyapunov well 'restricting' r in $(-\bar{r}, \bar{r})$ (see Figure 6). Therefore, the controller constrains $\hat{\alpha}_1$, $\hat{\alpha}_2$, $\hat{\alpha}_3$ and r such that $\inf_{t\geq 0}\hat{\alpha}_1 > 0$, $\inf_{t\geq 0}\hat{\alpha}_2 > 0$, $\inf_{t\geq 0}\hat{\alpha}_3 > 0$ and

$r(t) \in (-\bar{r}, \bar{r})$ for all $t \geq 0$. Therefore the mass never contacts either electromagnets.

Remark 4.2 In electrostatic actuation, we may want to ensure that $r(t) \in (-\bar{r}+\varepsilon, \bar{r}-\varepsilon)$ for all $t \geq 0$ where $\varepsilon > 0$ is a safety gap between the electrodes to prevent arcing. The controller presented in this section can be easily modified by replace $\bar{r}$ by $\bar{r}-\varepsilon$ in (20). The proof follows by modifying the Lyapunov well in (24) by replacing $\bar{r}$ by $\bar{r} - \varepsilon$.

Remark 4.3 The controller (13)-(21) can easily be modified for tracking time-varying commands. To see this, consider a bounded time varying command $r_{\text{comm}} : [0, \infty) \to (-\bar{r}, \bar{r})$. Let the tracking error be given by $\xi = r - r_{\text{comm}}$. Then equation (12) becomes

$$\ddot{\xi}+c\dot{\xi}+k\xi = -kr_{\text{comm}}+\frac{i_1^2}{\alpha_1(\bar{r}-r_{\text{comm}}-\xi)^2}-\frac{i_2^2}{\alpha_2(\bar{r}+r_{\text{comm}}+\xi)^2} \quad (27)$$

The controller essentially remains the same except that v is now given by

$$v \triangleq (\hat{c}-a_1)\dot{\xi}+(\hat{k}-a_2)\xi+\hat{\alpha}_3\,\text{sign}(P_{12}\xi+P_2\dot{\xi})-\frac{P_{12}r+P_2\dot{r}}{(\bar{r}-r)(\bar{r}+r)^{3/2}}. \quad (28)$$

It can be shown that $\xi(t)$, $\dot{\xi}(t) \to 0$ as $t \to \infty$. Furthermore, $r(t) \in (-\bar{r}, \bar{r})$ for $t \geq 0$ and $\dot{r}(t)$, $\hat{c}$, $\hat{k}$, $\hat{\alpha}_1$, $\hat{\alpha}_2$, and $\hat{\alpha}_3$ are bounded for all $t \geq 0$. Furthermore $\inf_{t\geq 0} \hat{\alpha}_1 > 0$, $\inf_{t\geq 0} \hat{\alpha}_2 > 0$ and $\inf_{t\geq 0} \hat{\alpha}_3 > 0$.

4.1 Numerical Simulation

Consider the double-sided ECO shown in Figure 5 with the dynamics given by (12). For numerical simulations we consider $m = 1.0$, $c = 4.0$, $k = 16.0$, $\bar{r} = 2.0$, $a_1 = 45.0$, $a_2 = 100.0$, $a = 2.5$, $b = 3.5$ and $R \triangleq \begin{bmatrix} 100 & 0 \\ 0 & 10 \end{bmatrix}$.

First, we consider disturbance rejection of the square-wave disturbance $f_d(t) = 250\text{square}(t)$. The results of the simulation (Figure 4.1, Figure 4.1) indicate that the control algorithm manages to reject the unknown time-varying disturbance and ensures non-contact of the mass and the electromagnet.

Next, we consider stabilizing the mass close to the right electromagnet. The desired set-point is chosen to be $r_{\text{eq}} = 1.99$. However, we also give the mass an initial 'push' towards the right electromagnet by choosing the initial conditions as $(r(0), \dot{r}(0)) = (0.0, 50.0)$. The simulation result (Figure 9, Figure 4.1) shows that the control algorithm is able to stabilize the system at $r = 1.99$. Figure 4.1 shows that the control input i_2 has to sharply 'cut-back' to avert the initial 'push' before settling to a constant stabilizing value.

5 Conclusion

In this paper, we developed robust controllers for electromagnetically controlled oscillators with single- and

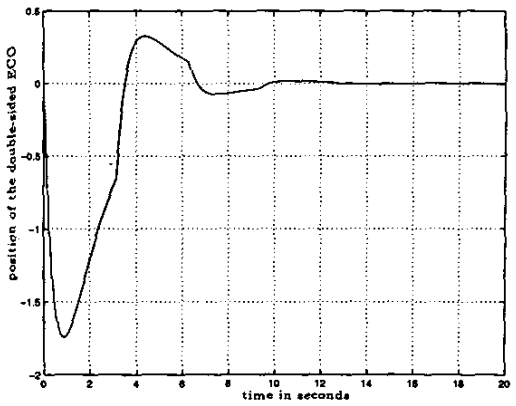

Figure 7: Time history of the mass position of the double-sided ECO subjected to the time-varying disturbance $f_d(t) = 250\,\text{square}(t)$.

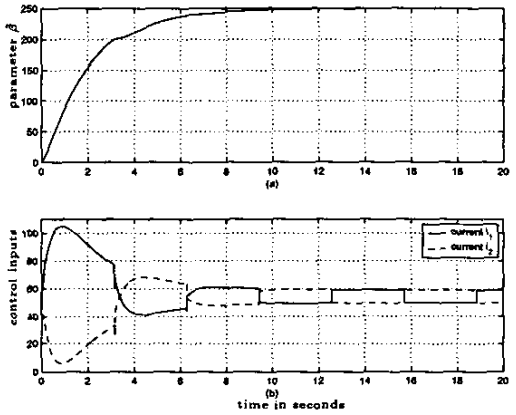

Figure 8: Time history of (a) the parameter $\hat{\alpha}_3$ and (b) the control currents i_1 and i_2 corresponding to the closed-loop response shown in Figure 4.1.

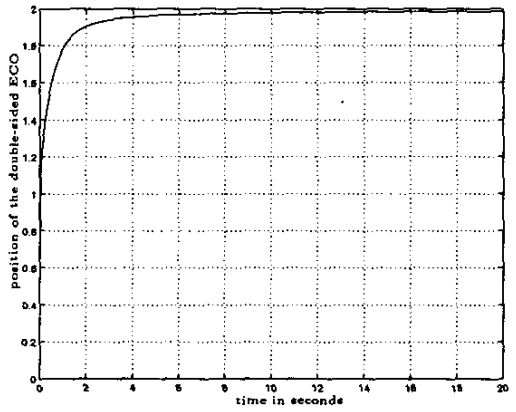

Figure 9: Time history of the mass position of the double-sided ECO for a step tracking command $r_{\text{eq}} = 1.99$.

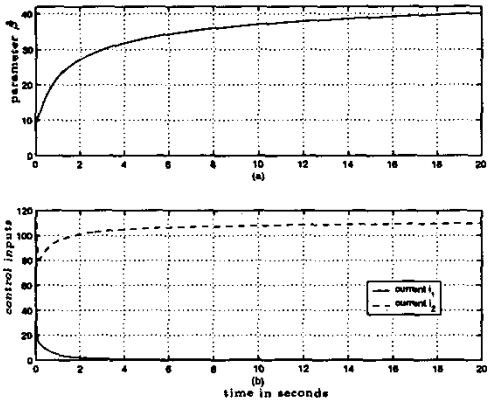

Figure 10: Time history of (a) the parameter $\hat{\alpha}_3$ and (b) the control currents i_1 and i_2 corresponding to the closed-loop response shown in Figure 9.

double-sided actuation. This problem is of particular importance in micro-electromechanical systems (MEMS) and eletromagnetically levitated systems. It is well known that a voltage driven parallel plate has a stable actuation range of one third of the nominal gap and linear controllers based on linearized models are unstable at large deflections. Due to the nonlinear dependence of the dynamics on the position and the control inputs, developing provably stable robust controllers for such systems presents a considerable challenge.

For Hammerstein systems with quadratic input nonlinearity Theorem 3.1 provides a nonlinear controller that guarantees stability and bounded disturbance rejection. For a single-sided ECO we use this controller to achieve tracking. For a double-sided ECO (Section 4), Theorem 4.1) provides a control algorithm that achieves the desired performance while guaranteeing that the electromagnetic plates never pull together. The method of proof is based on the concept of Lyapunov wells [15, 16] which in conjunction with the application of invariance principle guarantees the restriction of chosen variables to pre-defined intervals for all time. Remark 4.1 summarizes the idea briefly. These nonlinear controllers are robust since their stabilization and disturbance rejection properties do not require knowledge of the inertia, damping and stiffness of the plant.

References

[1] T. G. Bifano, J. Perreault, R. K. Mali, and M. N. Horenstein. Microelectromechanical deformable mirrors. *IEEE J. Select. Topics. Quant. Electonics.*, 5(1):83–89, January 1999.

[2] W. A. Clark. *Micromachined Vibratory Rate Gyroscopes.* PhD thesis, University of California, Berkeley, 1997.

[3] M. Elwenspoek and R. Wiegerink. *Mechanical Microsensors.* Springer, Berlin, 2001.

[4] L. S. Fan, H. H. Ottesen, T. C. Reily, and R. W. Wood. Magnetic recording-head positioning at very high track densities using microactuator-based, two stage servo system. *IEEE Trans. Ind. Electronics*, 42:222–233, June 1995.

[5] J. Hong and D. S. Bernstein. Experimental application of direct adaptive control laws for adaptive stabilization and command following. In *Proc. Conf. Dec. Contr.*, pages 779–783, Phoenix, AZ, December 1999.

[6] J. Hong, I. A. Cummings, D. S. Bernstein, and P. D. Washabaugh. Stabilization of an electromagnetically controlled oscillator. In *Proc. Amer. Contr. Conf.*, pages 2775–2779, Philadelphia, PA, June 1998.

[7] D. A. Horsley, A. Singh, R. Horowitz, and A. P. Pisano. Angular micropositioner for disk drives. In *Proc. 10th Intl. Conf. on MEMS*, pages 454–459, Nagoya, Japan, 1997.

[8] D. A. Horsley, N. Wongkomet, R. Horowitz, and A. P. Pisano. Precision positioning of microfabricated electrostatic actuator. *IEEE Trans. on Magnetics*, 35(2):993–999, March 1999.

[9] T. Imanura, T. Koshikawa, and M. Katayama. Transverse mode electrostatic microactuator for MEMS-based HDD slider. In *Proc. 9th Intl. Conf. on MEMS*, pages 216–221, San Diego, CA, 1996.

[10] T. N. Juneau. *Micromachined Dual Input Axis Rate Gyroscope.* PhD thesis, University of California, Berkeley, 1991.

[11] J. H. Lang and D. H. Staelin. Electrostatically figured reflecting membrane antennas for satellites. *IEEE Trans. Autom. Contr.*, 27:666–670, 1982.

[12] L. Y. Lin, E. L. Goldstein, and R. W. Tkach. Free-space micromachined optical switches for optical networking. *IEEE J. Select. Topics. Quant. Electonics.*, 5(1):4–9, January 1999.

[13] S. E. Lyshevski and M. A. Lyshevski. Analysis, dynamics and control of micro-electromechanical systems. In *Proc. Amer. Cntrl. Conf.*, pages 3091–3095, Chicago, IL, June 2000.

[14] D. J. Mihora and P. J. Redmond. Electrostatically formed antennas. *Journal of Spacecraft*, 17:465–475, 1980.

[15] H. Sane and D. S. Bernstein. Asymptotic disturbance rejection for Hammerstein systems with passive linear dynamics. In *Proc. Amer. Contr. Conf.*, pages 1449–1454, Arlington, VA, June 2001.

[16] H. S. Sane. *Adaptive Stabilization and Disturbance Rejection for Linear Systems and Hammerstein Systems.* PhD thesis, University of Michigan, Ann Arbor, 2001.

[17] J. I. Seeger and S. B. Crary. Stabilization of electrostatically actuated mechanical devices. In *Proc. Intl. Conf. on Solid-State Sensors and Actuators*, pages 1133–1136, Chicago, IL, June 1997.

[18] P. K. Sinha. *Electromagnetic Suspension: Dynamics and Controls.* Peter Peregrinus Ltd., London, 1987.

[19] N. Yazdi. *Micro-g Silicon Accelerometers with High Performace CMOS Circuitry.* PhD thesis, University of Michigan, Ann Arbor, 1999.

[20] N. Yazdi and K. Najafi. All-silicon single wafer micro-g accelerometer with combined surface and bulk micromachining process. *Journal of Microelectromechanical Systems*, 9(4):544–550, December 2000.